Supplemental material: Orbital edge states in a photonic honeycomb lattice

M. Milićević,[1] T. Ozawa,[2] G. Montambaux,[3,4] I. Carusotto,[2] E. Galopin,[1]
A. Lemaître,[1] L. Le Gratiet,[1] I. Sagnes,[1] J. Bloch,[1,4] and A. Amo[1]

[1] *Centre de Nanosciences et de Nanotechnologies, CNRS, Univ. Paris-Sud, Université Paris-Saclay, C2N - Marcoussis, 91460 Marcoussis, France*
[2] *INO-CNR BEC Center and Dipartimento di Fisica, Università di Trento, I-38123 Povo, Italy*
[3] *Laboratoire de Physique des Solides, CNRS, Univ. Paris-Sud, Université Paris-Saclay, 91405 Orsay Cedex, France*
[4] *Département de Physique, École Polytechnique, Université Paris Saclay, F-91128 Palaiseau Cedex, France*

(Dated: January 27, 2017)

SETUP AND EXPERIMENTAL CONDITIONS

To experimentally evidence the edge states wavefunctions and their dispersion relation we carry out low temperature (10K) luminescence experiments in reflection geometry. We excite the sample non resonantly using the CW monomode Ti:Saphire laser at 740nm wavelength, about 100 meV above the polaritonic bands, close to the fist reflection minimum of the cavity stop band. In this way we create electron-hole pairs that incoherently relax and populate all the polaritonic bands of the structure. Due to their finite lifetime polaritons escape the cavity in the form of photons whose energy and in-plane momentum correspond to those of the polaritons from which they originate. We collect the emitted photons using a high numerical aperture objective (NA=65), the same one used to focus the excitation beam. To distinguish between the real and momentum space imaging two variations of the setup are used. In the case of real space, the signal collected by the objective is magnified and directly imaged on the monochromator slit using a movable lens, see Fig. S1(a). The 1D slice of the image selected by the slit is then dispersed and imaged by a Peltier cooled CCD. Using a motorized translational stage, the position of the imaging lens is uniformly shifted such that the image of the whole lattice can be reconstructed, revealing the wavefunction distribution at different energies.

In order to reveal the dispersion of the edge states, angle resolved measurements have been performed by using an additional lens, see Fig. S1(b). Upon escaping the cavity photons emitted at the certain angle are all focused by the objective on the same point of Fourier plane. This plane is then imaged on the monochromator slit revealing the dispersion (far field imaging).

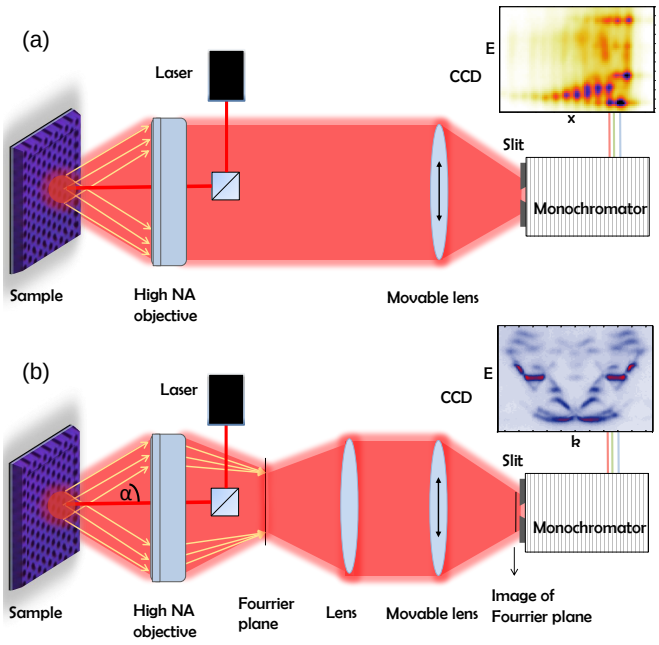

FIG. S1. Scheme of the experimental setup to measure energy selected real-space (a), and angle resolved –momentum sapce– (b) images.

P-BANDS HAMILTONIAN FOR A NANORIBBON

In the tight-binding calculations, we consider a p-orbital honeycomb lattice in a nanoribbon geometry: an infinite lattice in one direction and finite in the perpendicular one, ending with the same type of boundary on both sides. Ribbons with zigzag and bearded edges, infinite in the y-direction and finite in the x-direction, are shown in Fig. S2(a, b). The ribbon with armchair terminations is infinite in the x-direction and finite in the y-direction, Fig. S2(c). In order to include the information about the edges into the tight-binding Hamiltonian, we take a unit cell dimer such that the whole nanoribbon, with the specific type of the edge, can be reconstructed by the translation of that dimer [S1]. The unit cell dimers for the three different nanoribbons in Fig. S2(a-c) are shown in orange rectangles. The corresponding unit cell vectors can be chosen in the following way (green arrows

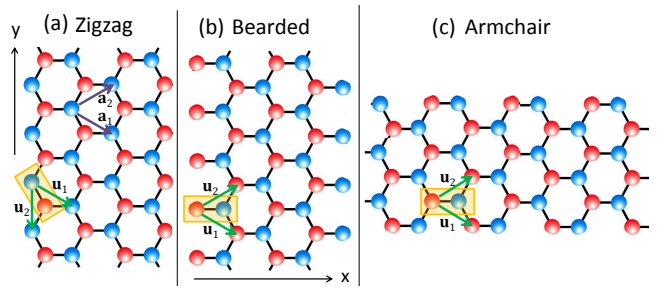

FIG. S2. Geometry of the honeycomb lattice ribbons with (a) zigzag, (b) bearded and (c) armchair edges, with the corresponding unit cell dimers and unit cell vectors.

in Fig. S2(a-c)):

$$\begin{aligned} bearded, armchair: \mathbf{u}_1 &= \mathbf{a}_1, \\ \mathbf{u}_2 &= \mathbf{a}_2, \\ zigzag: \mathbf{u}_1 &= \mathbf{a}_1, \\ \mathbf{u}_2 &= \mathbf{a}_1 - \mathbf{a}_2, \end{aligned} \tag{S1}$$

where $\mathbf{a}_1 = a(\frac{3}{2}, \frac{\sqrt{3}}{2})$ and $\mathbf{a}_2 = a(\frac{3}{2}, \frac{-\sqrt{3}}{2})$.

In the nearest neighbour approximation, the Hamiltonian is given by the factors f_1, f_2 and g [Eq.(1) in the main text] which have the following form [S2]:

$$\begin{aligned} f_1 &= \frac{3}{4}(e^{i\mathbf{k}\cdot\mathbf{u}_1} + e^{i\mathbf{k}\cdot\mathbf{u}_2}), \\ f_2 &= 1 + \frac{1}{4}(e^{i\mathbf{k}\cdot\mathbf{u}_1} + e^{i\mathbf{k}\cdot\mathbf{u}_2}), \\ g &= \frac{\sqrt{3}}{4}(e^{i\mathbf{k}\cdot\mathbf{u}_1} - e^{i\mathbf{k}\cdot\mathbf{u}_2}), \end{aligned} \tag{S2}$$

where $\mathbf{u}_1$ and $\mathbf{u}_2$ are given in Eq. (S1) for the three types of edges considered in the main text. The numerical factors in equations (S2) arise from the $|t_L| \gg |t_T|$ condition, which accounts for the different overlap between the p-orbitals projected along the directions parallel and perpendicular to the link between the lattice sites.

DRIVEN DISSIPATIVE TIGHT-BINDING SIMULATION

To understand the inhomogeneities that appear in the measured far field intensity in Fig.1(e-f) in the main text, we account the effect of photonic losses in the tight-binding lattice. This can be simulated by a Schrödinger equation of the form:

$$i\hbar\frac{\partial}{\partial t}\psi = \left(H - i\frac{\gamma}{2}\right)\psi + F_p e^{i\omega t}, \tag{S3}$$

where, H is the tight-binding Hamiltonian, γ represents the losses induced by the finite polariton lifetime, and F_p is a resonant pump at frequency ω and spatially centered on a single micropillar with a Gaussian envelope [S3]. We assume losses at a rate $\gamma = 0.2t_L$ for all lattice sites. To simulate the bulk luminescence we place the coherent pump F_p, with frequency ω, at the central site of the ribbon, far from the edges. We search for the steady-state solutions of Eq. (S3). The time-independent amplitudes $A_{m,n}$ and $B_{m,n}$ of the A and B sublattice sites (see Fig. S6) then satisfy a linear system of equations:

$$\begin{aligned} \hbar\left(\omega + i\frac{\gamma}{2}\right) A_{m,n} + tB_{m,n} + tB_{m-1,n-1} + tB_{m-1,n+1} &= f^{(A)}_{m,n} \\ \hbar\left(\omega + i\frac{\gamma}{2}\right) B_{m,n} + tA_{m,n} + tA_{m+1,n+1} + tA_{m+1,n-1} &= f^{(B)}_{m,n} \end{aligned} \tag{S4}$$

where $f^{(A/B)}_{m,n}$ is the spatial amplitude profile of the pump on the A/B site of unit cell m, n. To reconstruct the dispersion, the distribution obtained from the above equations is Fourier transformed and the procedure is repeated for different frequencies ω of the pump. Figure S3(a) shows the Fourier transformed intensity as a function of k_y for the value of $k_x = 4\pi/3a$ for different resonant pump frequencies. This result can be compared to the experimental data in the Fig. 1(e) of the main text, here replotted in Fig. S3(c). As we can see, the main features of the experiment are well reproduced by the simulation, including the destructive interference in the upper dispersive band around $k_y = 0$. This point crosses a high symmetry direction along which odd real-space eigenfunctions interfere destructively in the far field.

We perform a similar calculation with the excitation spot placed at the edge with the zigzag boundary instead of the central site of the lattice. The computed intensity pattern is plotted in Fig. S3(b), which reproduces well the experimental data in Fig. S3(d) [Fig. 1(f) in the main text] excluding the polarisation effects, which are not taken into account in this simulation.

MOMENTUM SPACE EMISSION ON THE ARMCHAIR EDGE

Similarly to the zigzag edge states dispersion shown in Fig. 1(f), we perform momentum space spectroscopy on the armchair edge. Figure S4(d) shows the emission from the edge states, which can be identified by comparing it with images when exciting the center of the lattice [Fig. S4(c)]. The dispersive edge modes are clearly visible between the flat bands. Note that the dark regions arise mainly from the destructuve interference along high symmetry directions described in the main text. This interference effects are also found in driven dissipative tight-binding simulations [Fig. S4(a),(b)].

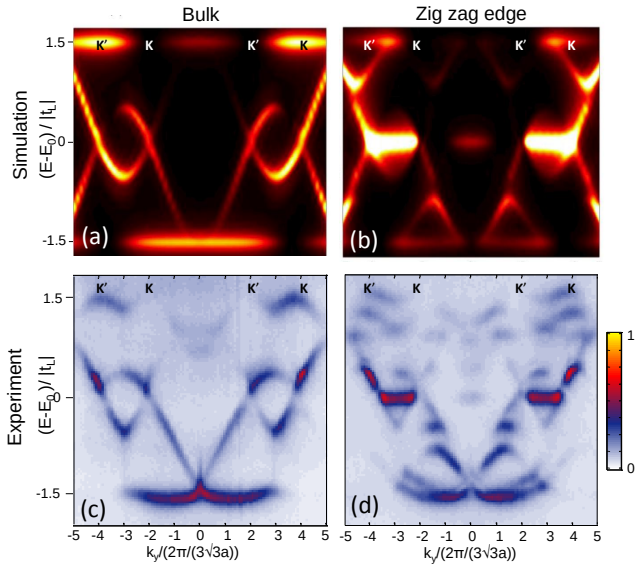

FIG. S3. (a-b) Momentum space distribution along the k_y direction for $k_x = 4\pi/(3a)$ obtained from a driven-dissipative tight-binding simulation when exciting the bulk (a) or the edge (b) of a ribbon with zigzag terminations. (c-d) Measured momentum-space luminescence for the same value of k_x for excitation in the bulk (c) and at the edge (b).

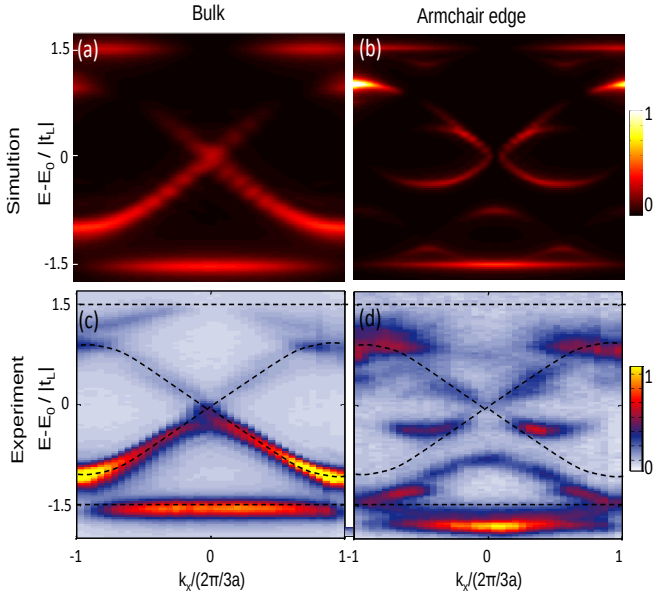

FIG. S4. (a-b) Momentum space distribution along the k_x direction for $k_y = -4\pi/(3\sqrt{(3)}a)$ obtained from a driven-dissipative tight-binding simulation when exciting the bulk (a) or the edge (b) of a ribbon with armchair terminations. (c-d) Measured momentum-space luminescence for the same value of k_y for excitation in the bulk (c) and at the edge (b).

WINDING NUMBER

For a Hamiltonian of the form $\begin{pmatrix} 0 & Q^\dagger \\ Q & 0 \end{pmatrix}$, where the matrix Q is defined in the main text [Eq. (1)], the number of pairs of zero-energy edge modes for a given value of $k_\parallel$ parallel to the edge is given by the winding of the phase of $\det Q$ along the direction perpendicular to the edge, the winding number, as discussed in detail in Refs. [S1, S4, S5]:

$$\mathcal{W}(k_\parallel) = \frac{1}{2\pi}\int_{BZ} \frac{\partial\phi\,(\mathbf{k})}{\partial k_\perp} dk_\perp, \qquad \text{(S5)}$$

where $\phi = \arg(\det Q)$, $k_\perp$ is the momentum directed perpendicularly to the considered edge, and BZ indicates a one-dimensional integral over the Brillouin zone. In Fig. S5, we plot the phase ϕ, represented by the orientation of the arrows at each point in k space, calculated for zigzag and bearded terminations for the s- [$\arg(\det f_s)$] and p-states [$\arg(\det f_p)$], where f_s and f_p are defined in the main text.

NUMERICAL CALCULATION OF EDGE STATES WAVEFUNCTION

Here we briefly discuss how Fig. 3 (d-f) of the main text are numerically calculated. In order to obtain the wavefunction localized at the armchair edge, we consider a nanoribbon with an infinite length in x-direction and a finite size in y-direction. We then diagonalize the nanoribbon Hamiltonian and find eigenstates corresponding to the edge states indicated in Fig. 2(c) of the main text. The obtained eigenstates are plane waves in the parallel direction, with wavevector $k_x = -\pi/3a$, $+\pi/3a$, and 0 [Fig. 3 (d), (e), and (f), respectively] and exponentially decaying in the perpendicular direction. For each eigenstate, the wavefunction at each site has two components corresponding to two orbital degrees of freedom. For concreteness, let the spinor (ψ_x, ψ_y) denote the wavefunction of a site at the origin in basis of p_x and p_y orbitals. In order to plot the wavefunction corresponding to this spinor, we assume that the x-oriented basis state is proportional to $\phi_x(x,y) \equiv x \cdot e^{-(x^2+y^2)/2\sigma^2}$, where the factor of x in front ensures that the state has the correct odd parity of the p_x orbital state around $x = 0$ (center of the pillar). The subsequent Gaussian has one free parameter σ, which determines the width of the state; we use $\sigma = 0.35a$ for all the calculations, which is chosen so that the simulation resembles the experimentally observed real space emission. Similarly, the y-oriented basis state is chosen to be $\phi_y(x,y) \equiv y \cdot e^{-(x^2+y^2)/2\sigma^2}$. The real space wavefunction corresponding to the spinor (ψ_x, ψ_y) is $\psi_x\phi_x(x,y) + \psi_y\phi_y(x,y)$. We construct the wavefunction of each lattice site with this method and superpose the wavefunctions from all lattice sites in the region of interest to finally obtain the wavefunction corresponding to the eigenstates, which are plotted in Fig. 3 (d-f).

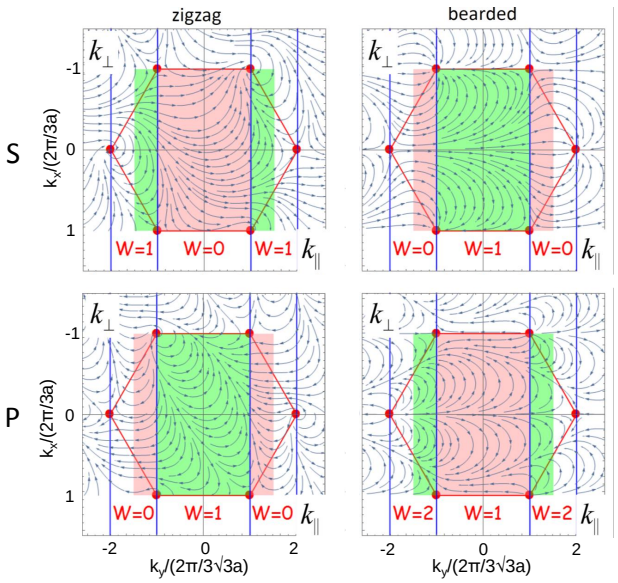

FIG. S5. Winding of the phase $\phi(\mathbf{k})$ for s-band graphene (top row) and orbital p-band graphene (bottom rows). The winding number $\mathcal{W}(k_\parallel)$ is indicated, $k_\parallel$ being the direction of the wave vector along the edge. The colored region is a rectangular Brillouin zone. In the pink regions, the winding number $\mathcal{W}$ is even while it is odd in the green regions. Both in s- and p-bands, the regions in momentum of existence of edge states are complementary between the zigzag and bearded edges. Additionally, they are complementary between s- and p-bands for the same kind of edge. There is an additional p-edge state at the bearded edge for all values of $k_\parallel$, resulting in an additional winding of the phase.

ANALYTICAL EXPRESSIONS FOR THE ENERGY OF THE DISPERSIVE EDGE STATES

To obtain the analytical expressions for the energy of the dispersive, non-zero energy edge states in zigzag and bearded edges we look for the exponentially decaying solutions of the tight-binding Hamiltonian of a nanoribbon. To illustrate the procedure we apply it first to the simpler case of s-bands graphene [S6]. The first step is to reduce the two-dimensional problem of a nanoribbon to an equivalent one-dimensional problem, that is, to reduce our s-band honeycomb problem to the SSH problem. The Hamiltonian of the nanoribbon in Fig. S6 is given by:

$$H = -t_s \sum_{\text{m-n is even}} \Big(a^\dagger_{m,n} b_{m,n} + a^\dagger_{m+1,n+1} b_{m,n} + a^\dagger_{m+1,n-2} b_{m,n} + h.c. \Big) \quad \text{(S6)}$$

To solve the Schrödinger equation $H|\Psi\rangle = E|\Psi\rangle$ we expand the state $|\Psi\rangle$ in terms of the creation operators

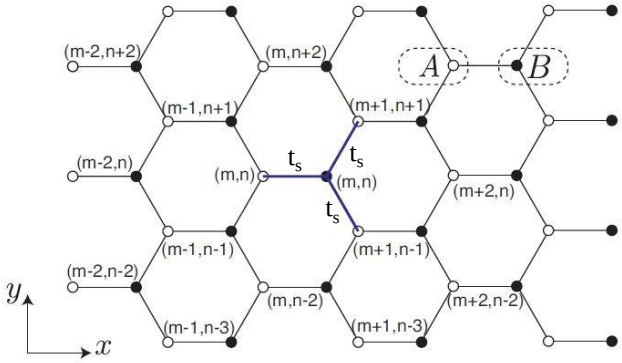

FIG. S6. Graphene nanoribon with bearded edges

as:

$$|\Psi\rangle = \sum_{\text{m-n is even}} \Big(A_{m,n} a^\dagger_{m,n} + B_{m,n} b^\dagger_{m,n} \Big) |0\rangle \quad \text{(S7)}$$

where $|0\rangle$ is the state without any particle in the system. The coefficients $A_{m,n}$ and $B_{m,n}$ represent the wavefunctions in A and B sublattices at the position (m,n). Using this expression for $|\Psi\rangle$, the Schrödinger equation implies the following relations for the coefficients $A_{m,n}$ and $B_{m,n}$:

$$\begin{aligned} -t_s(B_{m,n} - B_{m-1,n-1} - B_{m-1,n+1}) &= E A_{m,n} \\ -t_s(A_{m,n} - A_{m+1,n+1} - A_{m+1,n-1}) &= E B_{m,n}. \end{aligned} \quad \text{(S8)}$$

For a nanoribbon with bearded or zigzag edge the system is periodic (or infinitely long) along the y-direction. That means that we can expand the wavefunctions in terms of the plane wave in y-direction, i.e., we replace the wavefunctions in (S8) by:

$$A_{m,n} = e^{i\frac{\sqrt{3}}{2}ak_y n} A_m \qquad B_{m,n} = e^{i\frac{\sqrt{3}}{2}ak_y n} B_m \quad \text{(S9)}$$

In this way we obtain the equations:

$$\begin{aligned} -t_s(B_m - (e^{-i\frac{\sqrt{3}}{2}ak_y} + e^{i\frac{\sqrt{3}}{2}ak_y}) B_{m-1}) &= E A_m \\ -t_s(A_m - (e^{-i\frac{\sqrt{3}}{2}ak_y} + e^{i\frac{\sqrt{3}}{2}ak_y}) A_{m+1}) &= E B_m \end{aligned} \quad \text{(S10)}$$

If we define $\alpha \equiv (e^{-i\frac{\sqrt{3}}{2}ak_y} + e^{i\frac{\sqrt{3}}{2}ak_y}) = 2\cos(\frac{\sqrt{3}}{2}ak_y)$ these equations can be written as :

$$-t_s \begin{pmatrix} \ddots & & & & & & \\ & 0 & 1 & 0 & 0 & 0 & 0 \\ & 1 & 0 & \alpha & 0 & 0 & 0 \\ & 0 & \alpha & 0 & 1 & 0 & 0 \\ & 0 & 0 & 1 & 0 & \alpha & 0 \\ & 0 & 0 & 0 & \alpha & 0 & 1 \\ & 0 & 0 & 0 & 0 & 1 & 0 \\ & & & & & & \ddots \end{pmatrix} \begin{pmatrix} \vdots \\ A_{m-1} \\ B_{m-1} \\ A_m \\ B_m \\ A_{m+1} \\ B_{m+1} \\ \vdots \end{pmatrix} = E \begin{pmatrix} \vdots \\ A_{m-1} \\ B_{m-1} \\ A_m \\ B_m \\ A_{m+1} \\ B_{m+1} \\ \vdots \end{pmatrix} \quad \text{(S11)}$$

This set of equations has the same form as the Schrödinger equation describing a one dimensional chain with staggered hopping amplitudes (the so-called SSH model). The hopping amplitude within the unit cell dimer, t_s, is the same as the one in the honeycomb lattice in Fig. S7. The effective hopping amplitude between adjacent unit cell dimers in the chain is αt_s. The Hamiltonian of the system is given by the matrix on the left-hand side of the Eq. (S11). The difference between bearded and zigzag case is that, to calculate the bearded edge, one starts from the A sublattice and ends at the B sublattice. For the zigzag, one starts from the B sublattice and ends at the A sublattice.

Now, we search for eigenvalues of this Hamiltonian corresponding to eigenfunctions which are exponentially decaying into the bulk: $|A_M| = |A_0| e^{\frac{-3a}{2\xi} M} \equiv |A_0||\Omega|^M$. Here A_0 is the amplitude of the wavefunction on the first site of the chain, M counts the number of unit cells from the edge and ξ is the penetration length. In order to have a decaying wavefunction, we need to have $|\Omega| < 1$. Analogue expressions can be written for the B sites. Figure S7 shows bearded and zigzag ribbons and the equivalent 1D chains, with corresponding hopping and wavefunction amplitudes for the edge states.

After imposing the exponentially decaying solution to the problem, the Schrödinger equation for bearded edges has the form:

$$-t_s \begin{pmatrix} 0 & 1 & 0 & 0 & 0 & 0 & \\ 1 & 0 & \alpha & 0 & 0 & 0 & \\ 0 & \alpha & 0 & 1 & 0 & 0 & \\ 0 & 0 & 1 & 0 & \alpha & 0 & \\ 0 & 0 & 0 & \alpha & 0 & 1 & \\ 0 & 0 & 0 & 0 & 1 & 0 & \\ & & & & & & \ddots \end{pmatrix} \begin{pmatrix} A_0 \\ B_0 \\ A_0\Omega \\ B_0\Omega \\ A_0\Omega^2 \\ B_0\Omega^2 \\ \vdots \end{pmatrix} = E \begin{pmatrix} A_0 \\ B_0 \\ A_0\Omega \\ B_0\Omega \\ A_0\Omega^2 \\ B_0\Omega^2 \\ \vdots \end{pmatrix} \tag{S12}$$

This system of equations has four unknowns: A_0, B_0, Ω and E. However, we can normalize the wavefunction to the amplitude A_0 of the outermost site. Therefore we have only three unknowns left. They can be found by taking the first three equations from the set of equations (S12):

$$\begin{aligned} \epsilon A_0 &= t_s B_0 \\ \epsilon B_0 &= t_s A_0 (1 + \alpha\Omega) \\ \epsilon A_0\Omega &= t_s B_0 (\alpha + \Omega) \end{aligned} \tag{S13}$$

All the other equations contained in Eq.(S12) are equivalent to the set (S13). Using the condition $|\Omega| < 1$ we obtain the regions in momentum space where the zero energy edge states exist, Ref. [S6]. For the bearded edge we have $B_0 = 0$ and:

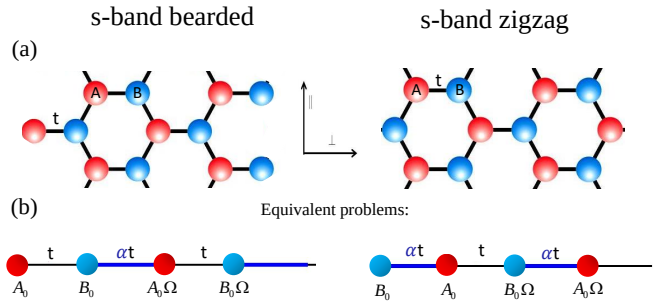

FIG. S7. (a) s-bands honeycomb lattice nanoribbons with bearded and zigzag edges (b) Equivalent dimer chains. Hopping amplitudes are given on the links between the chain sites, and amplitudes of the edge states wave functions below the chain sites.

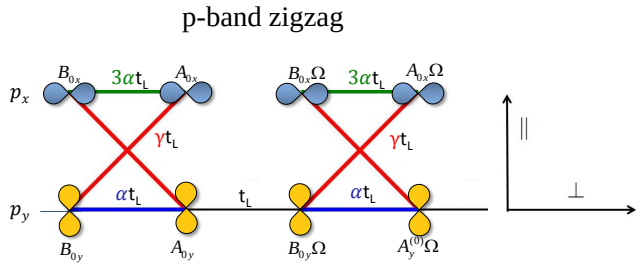

FIG. S8. Amplitudes of the wave function for zigzag nanoribbon in the p-band: the problem is reduced to two coupled dimer chains.The hopping amplitudes are given on the links between the chain sites.

$$\Omega = \frac{-1}{\alpha} = \frac{-1}{2\cos(\frac{\sqrt{3}}{2}ak_y)}$$
$$2|\cos\frac{\sqrt{3}}{2}ak_y| > 1 \tag{S14}$$

corresponding to the region marked in green in the upper-right panel of Fig. S5.

To obtain expressions for the energies of the dispersive edge states in the p-bands we follow the same procedure. In this case, due to the existence of two modes per site, the reduction to the 1D problem involves two coupled chains corresponding to the p_x and p_y orbitals on each lattice site. Figure S8 shows the hopping amplitudes corresponding to a ribbon with zigzag edges.

We search again for exponentially decreasing solutions of the form $|A_{Mx}| = |A_{0x}||\Omega|^M$ with $|\Omega| < 1$ (equivalently for $|A_{My}|$, $|B_{Mx}|$, $|B_{My}|$). Now we have six unknown variables $A_{0x}, A_{0y}, B_{0x}, B_{0y}, \Omega, E$ or five after we normalize them to B_{0y}. By taking the first five linear equations of the the Schrödinger problem, we get the set of coupled equations:

$$\begin{aligned}
\epsilon B_{0y} &= t_L(\gamma A_{0x} + \alpha A_{0y}) \\
\epsilon B_{0x} &= t_L(3\alpha A_{0x} + \gamma A_{0y}) \\
\epsilon A_{0x} &= t_L(3\alpha B_{0x} + \gamma^* B_{0y}) \\
\epsilon A_{0y} &= t_L(\alpha B_{0y} + \gamma^* B_{0x} + \Omega B_{0y}) \\
\epsilon B_{0y}\Omega &= t_L(A_{0y} + \alpha A_{0y}\Omega + \gamma A_{0x}\Omega)
\end{aligned} \tag{S15}$$

The energy of the dispersive edge state in the zigzag edge is obtained by solving Eqs. (S15) and is given by:

$$E^{zig}_{disp.edge}(k_\parallel) = \pm t_L \frac{\sqrt{3}}{2}\sqrt{2+\cos(\sqrt{3}k_\parallel a)}. \tag{S16}$$

The penetration length ξ can be easily obtained:

$$\begin{aligned}
\Omega &= \cos(\frac{\sqrt{3}}{2}k_\parallel a) \\
\xi &= -\frac{3a}{2\ln\left[\cos(\frac{\sqrt{3}}{2}k_\parallel a)\right]}.
\end{aligned} \tag{S17}$$

The amplitudes of the dispersive edge states eigenfunctions on the unit cell located at the edge are:

$$\begin{aligned}
A_{0x} = \mp\frac{i}{\sin(\frac{\sqrt{3}}{2}k_\parallel a)}\sqrt{\cos(\frac{\sqrt{3}}{2}k_\parallel a)+2} \quad &, \quad A_{0y} = 0 \\
B_{0x} = -i\sqrt{3}\cot(\frac{\sqrt{3}}{2}k_\parallel a) \quad &, \quad B_{0y} = 1
\end{aligned} \tag{S18}$$

where $\mp$ for the A_{0x} coefficient applies, respectively, to the positive/negative energy dispersive states.

Similar expressions describing the energy of the dispersive edge state in bearded edges [Eq.(8) in the main text], can be found in the same way.

[S1] P. Delplace, D. Ullmo and G. Montambaux, Phys. Rev. B **84**, 195452 (2011).

[S2] C. Wu and S. Das Sarma, Phys. Rev. B **77**, 235107, (2008).

[S3] T. Ozawa, and I. Carusotto, Phys. Rev. Lett. **13**, 133902 (2014).

[S4] S. Ryu and Y. Hatsugai, Phys. Rev. Lett. **89**, 077002 (2002).

[S5] R. S. K. Mong and V. Shivamoggi, Phys. Rev. B **83**, 125109 (2011).

[S6] M. Bellec, U. Kuhl, F. Mortessagne and G. Montambaux, New J. Phys. **16**, 113023 (2014).